九州大学学術情報リポジトリ
Kyushu University Institutional Repository

ベースプレートを省略した鉄筋内蔵コンクリート充填角形鋼管柱脚の力学的性状に関する実験的研究

喬, 崎雲
九州大学大学院人間環境学府空間システム専攻博士後期課程

松尾, 真太朗
九州大学大学院人間環境学研究院都市・建築学部門

尾園, 正樹
九州大学大学院人間環境学府空間システム専攻修士課程

陳, 思遠
九州大学大学院人間環境学府空間システム専攻修士課程

他

https://doi.org/10.15017/26752

出版情報：都市・建築学研究. 20, pp.111-117, 2011-07-15. 九州大学大学院人間環境学研究院都市・建築学部門
バージョン：
権利関係：

都市・建築学研究　九州大学大学院人間環境学研究院紀要　第20号，2011年7月
J. of Architecture and Urban Design, Kyushu University, No.20, pp.111～117, July. 2011

ベースプレートを省略した鉄筋内蔵コンクリート充填角形鋼管柱脚の力学的性状に関する実験的研究

An Experimental Study on Mechanical Behaviors of Non Base-plate Column Bases of Square CFTs with Built-in Reinforcements

喬　崎雲*，松尾真太朗**，尾園正樹***，陳　思遠***，野津手崇瑛***，蜷川利彦**，河野昭彦**
Qiyun QIAO*, Shintaro MATSUO**, Masaki OZONO***, Siyuan CHEN***,
Takaaki NOTSUTE***, Toshihiko NINAKAWA** and Akihiko KAWANO**

In this study, the authors propose a new exposed-type column base which is a non base-plate square CFT column base with built-in high strength reinforcements (square CFTR column base). The base plate and anchor bolts are omitted in this CFTR column base, but the high strength reinforcements are inserted from the CFT column to the RC foundation. A total of three specimens was fabricated. The parameter for the study is the axial force ratio (0, 0.25, 0.50). The specimens were tested under the horizontal cyclic lateral load while subjected to a constant axial load. The mechanical behaviors of the column bases are investigated. The test results indicate that the non base-plate CFTR column bases have excellent seismic performances and are applicable in the practical structural design.

Keywords : *CFTR Column Bases, High Strength Reinforcements, Stress Transfer Mechanism, Ultimate Bending Strengths*
CFTR 柱脚，高強度鉄筋，応力伝達機構，終局曲げ耐力

1. INTRODUCTION

The authors have carried out a series of studies on the connection of the concrete filled steel tube (CFT) with built-in reinforcements. In the series of studies, the mechanical behaviors of the column bases and column joints have been investigated. [1), 2), 3)]

This study, which is one part of the series of studies, focuses on the mechanical behaviors of the column bases. With regard to the usual exposed-type CFT column bases, the full penetration welding is necessary between the columns and the base plates. On the other hand, by inserting the reinforcements into the usual exposed-type CFT column bases, the welding work can be reduced, or in some cases, no weld is needed because of the omission of the base plates and the anchor bolts. In reference 4, the authors investigated the mechanical behaviors of the non base-plate circular CFT column bases with built-in reinforcements (circular CFTR column bases), and it was proved that the non base-plate circular CFTR column bases had excellent mechanical behaviors. However, when the CFT column type changes from circular to square sections, some mechanical conditions (especially the confinement between the steel tube and infill concrete) are different. Hence, it is necessary to investigate the behaviors of the non base-plate square CFT column base with built-in reinforcements (square CFTR column base).

In this study, the experiment on thenon base-plate square CFTR column bases was carried out. A total of three specimens was fabricated and tested. Based on the experiment, the mechanical behaviors of the non base-plate square CFTR column bases are investigated, and a strength evaluation method is proposed.

*　空間システム専攻・博士後期課程
**　都市・建築学部門
***　空間システム専攻・修士課程

2. SPECIMENS

Table 1 shows the summary of the test specimens. Figs.1(a) to (d) show the details of the specimens. As shown in Table 1 and Fig.1, the high strength reinforcements (USD685) were inserted through the CFT column to the foundation. The

anchorage length of the built-in reinforcements into the CFT column was 40D (D is the diameter of the reinforcing bars), which was thought as the enough length to avoid the slip of the built-in reinforcements. The square steel tubes had the dimensions of 300mm×300mm×6mm. Two rib bands were welded inside of the steel tube near the foundation. The rib bands were expected to be the mechanical shear keys between the steel tubes and infill concrete. A 10mm clearance was located between the steel tube and the foundation, so that the stress was ensured not to transfer from the steel tube to the foundation directly. In this way, the axial stress in the steel tube was firstly transferred to the infill concrete by the rib bands, then transferred from the concrete to the built-in reinforcements by the bond, and finally transferred to the foundation. A total of three specimens was tested under the reversed cyclic horizontal load while subjected to the constant axial load. The parameter for the test was the axial force ratio ($n=N/N_u$=0, 0.25, 0.50, where N is the axial load and N_u is the critical axial strength as defined in Eq.(1).

$$N_u = \sigma_y \cdot A_s + {}_c\sigma_B \cdot A_c \qquad (1)$$

A_s : Cross sectional area of the steel tube
σ_y : Yield stress of the steel tube
A_c : Cross sectional area of infill concrete
${}_c\sigma_B$: Maximum stress of the concrete

The average of the maximum stress of concrete ${}_c\sigma_B$ (cylinder strength) is shown in Table 1, and the steel material properties is shown in Table 2.

3. TEST PROCEDURE

Test setup is shown in Fig.2. The reversed cyclic horizontal load Q was applied by a 1000kN capacity hydraulic jack and the constant axial load N was maintained by a 5000kN capacity universal testing machine. As shown in Fig.3, the horizontal load was applied, so that the joint translation angle R ($R=u/L$, where u denotes the horizontal displacements and L is the distance from the surface of the foundation to the horizontal loading point) was taken from ±0.5% to ±3.0%, with two cycles in each amplitude of the R. After these loading procedures, the horizontal load was increased until 5.0% of the R monotonically.

Table 1 Summary of test specimens

Specimen	Steel Tube		Built-in Reinforcements		Axial Force Ratio ※1	Concrete Strength(N/mm^2)	
	Dim.(mm)	B/t	Quantity	Grade		Column	Foundation
No.1	□300×6	50	16-D19	USD685	0	64	69
No.2					0.25		
No.3					0.5		

※1. Axial force ratio was decided according to the compressive strength of the CFT column

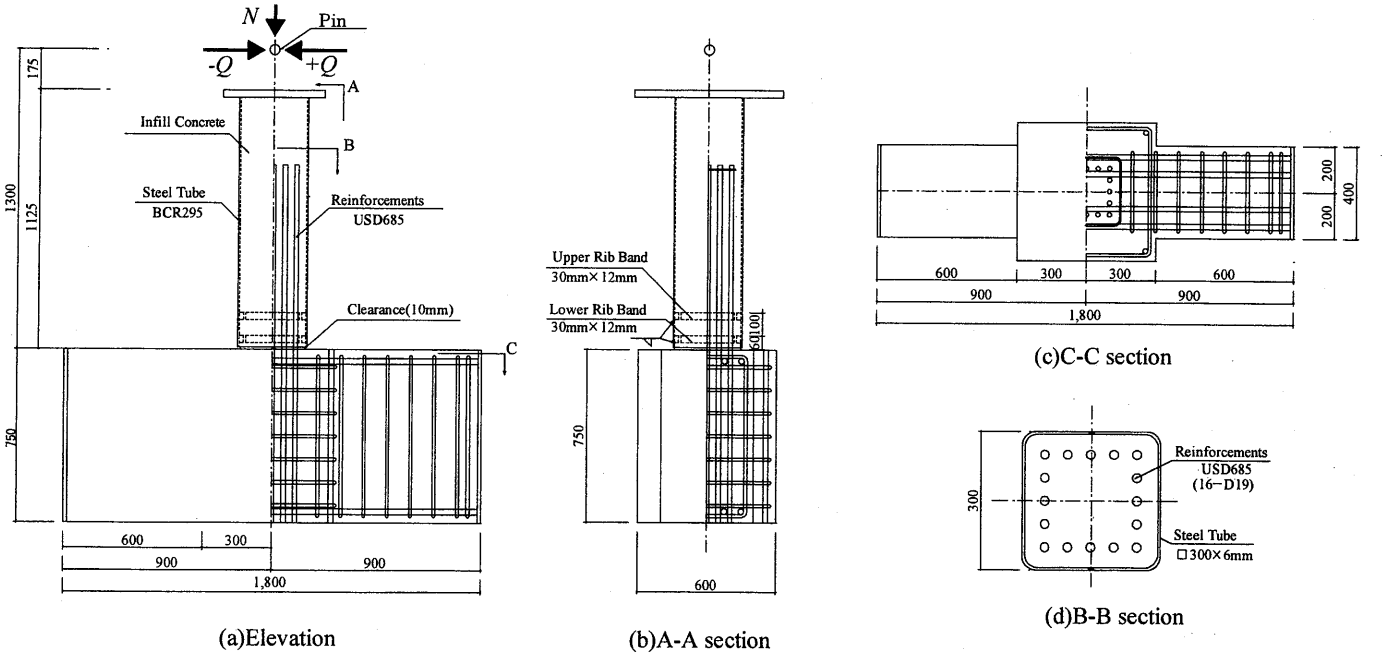

Fig.1 Details of the specimens

Table 2 Steel material properties

Steel Material	Grade	Young's Modulus ($\times 10^3$ N/mm^2)	Yield Strength (N/mm^2)	Tensile Strength (N/mm^2)	Yield Strain (%)	Elongation (%)
Steel Tube	BCR295	207	386	464	0.19	34.5
Reinforcements	USD685	197	694·	893	0.36	10.3

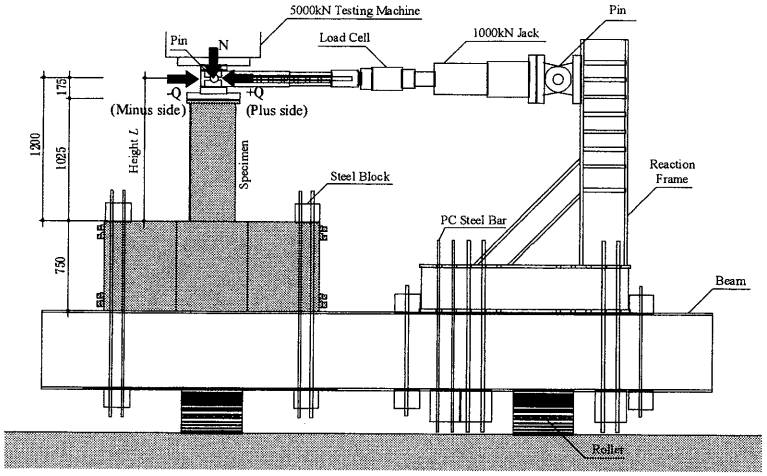

Fig.2 Test setup

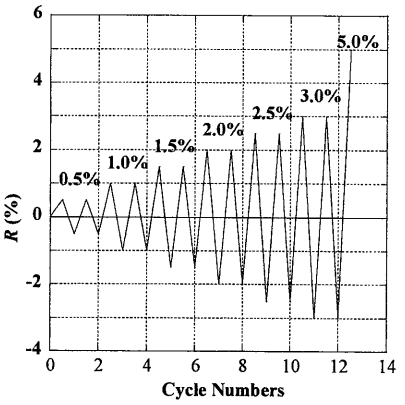

Fig.3 Loading program

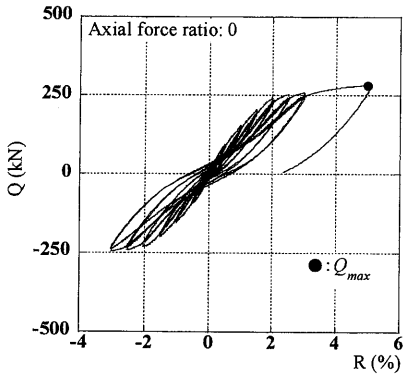

(a) No.1

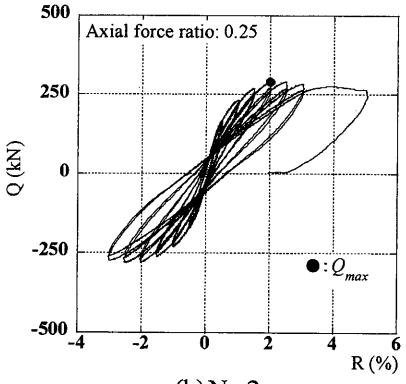

(b) No.2

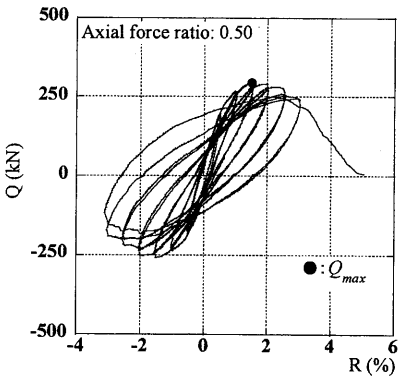

(c) No.3

Fig.4 *Q-R* relationships

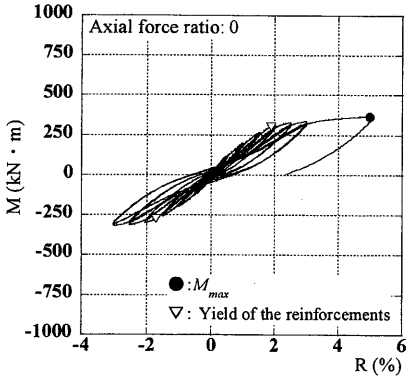

(a) No.1

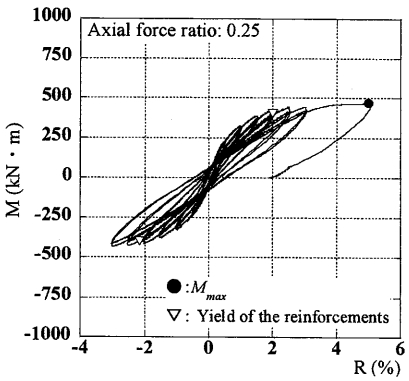

(b) No.2

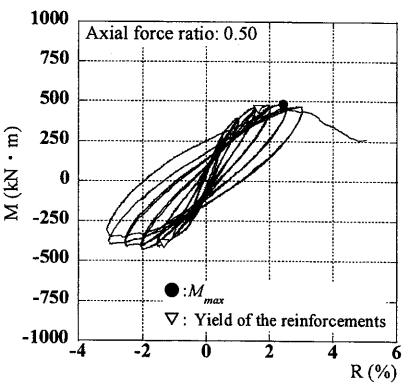

(c) No.3

Fig.5 *M-R* relationships

The longitudinal strain gauges were used in the several places of the reinforcements and the steel tubes. The longitudinal and horizontal relative displacements between the bottom of steel tube and the the foundation were also measured by the displacement transducers.

4. TEST RESULTS AND INVESTIGATIONS

4.1 Horizontal load Q and joint translation angle R relationship

Figs.4(a) to (c) show the relationships between the horizontal load Q and joint translation angle R. The symbol ● shows the maximum value of the horizontal load Q. The peak of the Q in each hysteresis loop of specimen No.1 increases as the amplitude of the R increases. As for specimens No.2 and No.3, the Q reaches the maximum strength when the amplitude of the R is from 1.5% to 2.0%. However, the load Q does not degrade rapidly with 3.0% of the amplitude of the R.

4.2 Bending moment M and joint translation angle R relationship

Figs.5(a) to (c) show the relationships between the bending moment of the column base M and joint translation angle R. The symbol ● shows the maximum bending moment of the column base and ▽ shows the yielding of the reinforcements.

With regard to the specimens No.1 and No.2 [Figs.5(a) and (b), respectively], the peak of the M in each hysteresis loop increases as the amplitude of the R increases. As for the specimen No.3 [(Fig.5(c)], the M reaches the maximum when the amplitude of the R is around 2.5%. It is proved that the deformation performances of these column bases are stable.

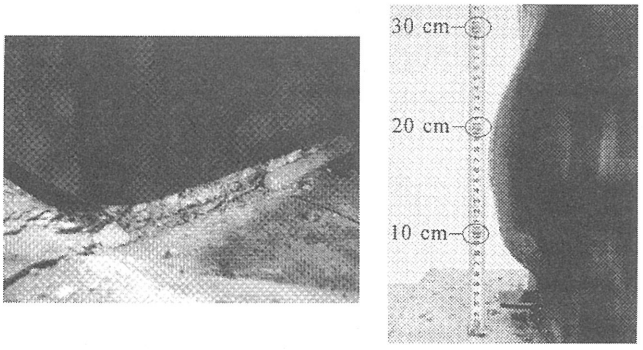

(a) Crush of the concrete (b) Local buckling

Fig.6 Fracture modes

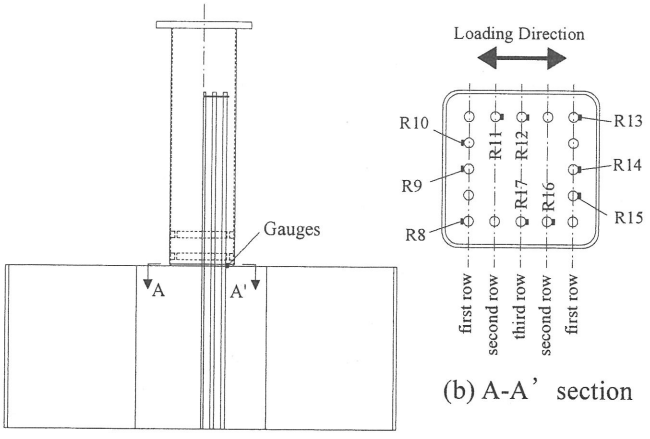

(a) Elevation (b) A-A' section

Fig.7 Numbering of the gauges

4.3 Fracture mode

The crack of concrete in the 10mm clearance part at the bottom of the column was caused by bending moments in the early loading steps. Finally, the crush was observed in the concrete as shown in Fig.6(a). As shown in Fig.6(b), the local buckling occurred in the steel tube of the specimen No.3 (n = 0.5) when the R reached around 3.0%. Two reasons of the local buckling may be considered for the specimen No.3. The first one is the B/t ratio of the steel tube is 50, which means the wall thickness of the steel tube is not large. The second one is the high axial force applied to the specimen No.3. In order to avoid the local buckling, one possible method is to add the hoop reinforcements inside the CFT column. In reference 4, the authors used the spiral hoops inside the circular CFT column. The D/t ratio of the circular steel tube was 97.5, and the high axial force ratio (n=0.45) was adopted for one of the specimens. However, no local buckling occurred at the circular CFTR specimens. Hence, in the occasion of the square CFT column, the hoop reinforcements may be effective in avoiding the local buckling. However, since some mechanical conditions are different for the square type and the circular type, it is necessary to further investigate the method of adding the hoop reinforcements into the square CFT column.

4.4 Strain characteristics of the built-in reinforcements

Fig.7 shows the numbering of the gauges installed in the built-in reinforcements at the base portion. Figs.8, 9, 10 show the relationships between the strains in the reinforcements at the base portion and joint translation angle R. A strain in tension is defined as positive. The average strain is adopted for the first row strain. The solid horizontal lines in the figures indicate the yield strain levels in tension and compression of the reinforcements. As shown in Fig.8, with regard to the specimen No.1 with axial force ratio of 0, it is found that the strains in the reinforcements of the first row and the second row reach the tensile yield strain level, but any of the strains in the reinforcements do not reach the compressive yield strain level. Fig.9 shows the results of the specimen No.2 with axial force ratio of 0.25, it is confirmed that the strains in the first row reinforcements reach the yield strain levels in tension and compression. The strains at the second nor third rows do not exceed the yield strain level. Fig.10 shows the results of the specimen No.3 with axial force ratio of 0.50. Any of the strains

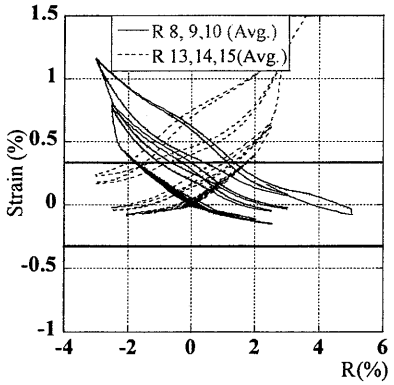

(a) First row of reinforcements

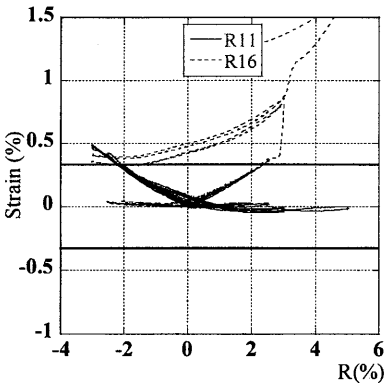

(b) Seccond row of reinforcements

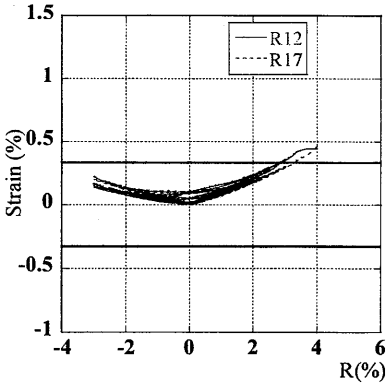

(c) Third row of reinforcements

Fig.8 Strain characteristics (Spceimen No.1)

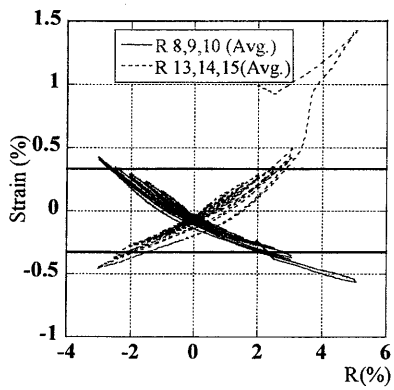

(a) First row of reinforcements

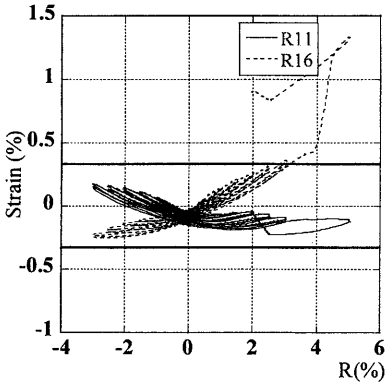

(b) Seccond row of reinforcements

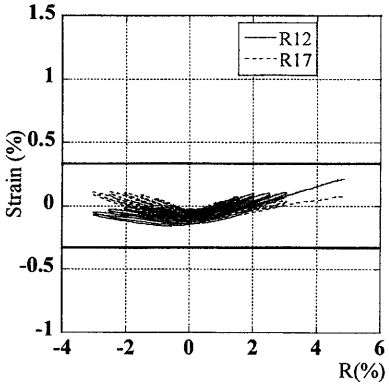

(c) Third row of reinforcements

Fig.9 Strain characteristics (Spceimen No.2)

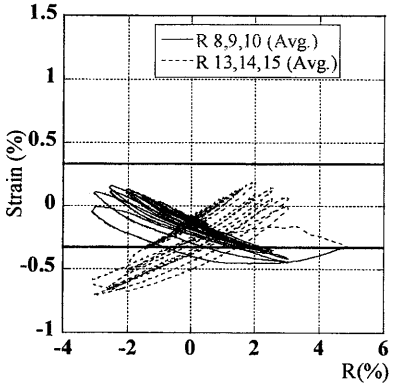

(a) First row of reinforcements

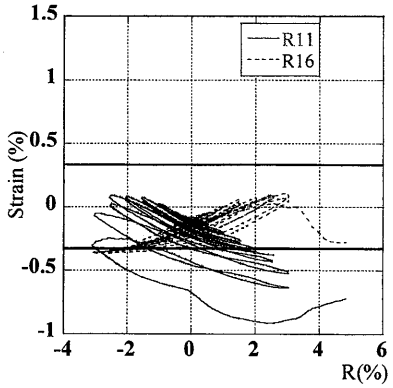

(b) Seccond row of reinforcements

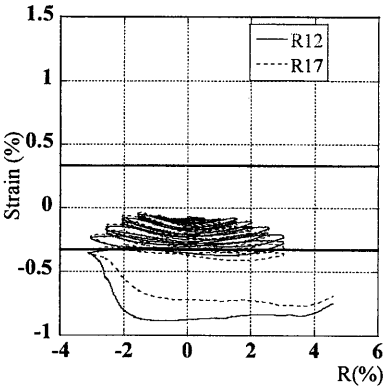

(c) Third row of reinforcements

Fig.10 Strain characteristics (Spceimen No.3)

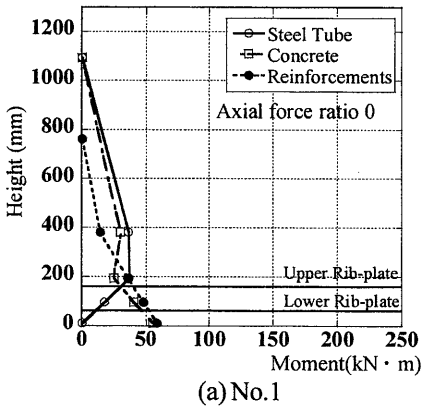

(a) No.1

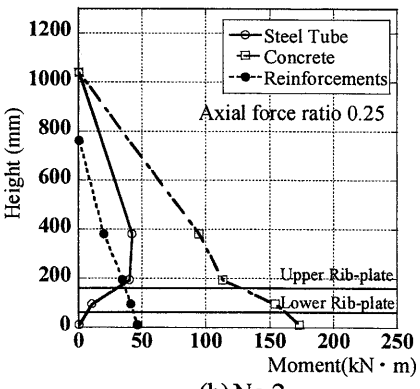

(b) No.2

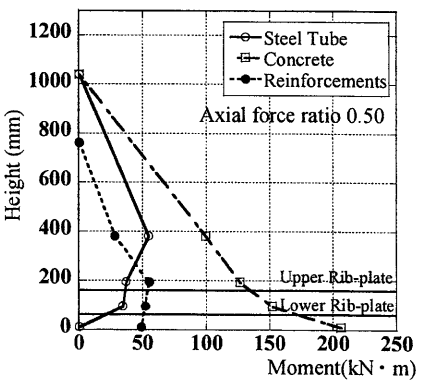

(c) No.3

Fig.11 Share conditions of the bending moments (R=0.5%)

do not exceed the tensile yield strain level, but exceed the compressive yield strain level. Also, as for the third row strains, it is observed that the compressive strains are cumulated with the cyclic loading process.

4.5 Stress transfer mechanism

According to the longitudinal strains in the steel tubes and reinforcements, the bending moments shared by the steel tubes, reinforcements and concrete are calculated when the joint translation angle R is 0.5%. The stress of the steel tubes and reinforcements are calculated by multiplying the longitudinal strains by the measured elastic modulus of the steel tube and reinforcements. The Bernoulli-Euler's hypothesis is adopted in the calculation. The concrete contributions are calculated by subtracting the bending moments of the steel tubes and reinforcements from the total applied bending moments.

Figs.11(a) to (c) show the share conditions of the bending moments when the joint translation angle R is 0.5%. In Fig.11, the height 0mm represents the surface of the concrete foundation (base portion) and the height 1300mm represents the height of the loading point. The horizontal solid lines show the locations of the rib bands. From the height 200mm to 0mm, the bending moments shared by the steel tubes decrease gradually. This indicates that the stresses in the steel tubes are transferred to the concrete inside the steel tubes gradually by the rib bands. It is proved that the built-in reinforcements and the rib bands are well effective in the stress transfer from steel tube to concrete. Also, it is confirmed that the bending moment shared by the concrete increase, as the axial force ratio increases.

4.6 Ultimate bending strength

4.6.1 Calculating method

(1) CFT column shaft

The ultimate bending strengths of the CFT column shafts are calculated. According to the reference 5, the CFT cross section (without built-in reinforcements) is considered as under the conditions of full plastic as shown in Fig.12.

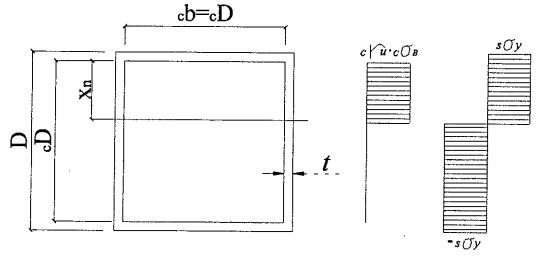

$_s\sigma_y$: Tensile yield stress $_c\sigma_B$: Cylinder strength

$_cr_u$: Concrete strength reduction factor =1.0

Fig.12 Stress distribution of the column shaft

(2) Column base

The ultimate bending strengths of the column bases are calculated according to the Fig.13 and Eq.(2). In the calculation, the cross section of column base section is considered as the

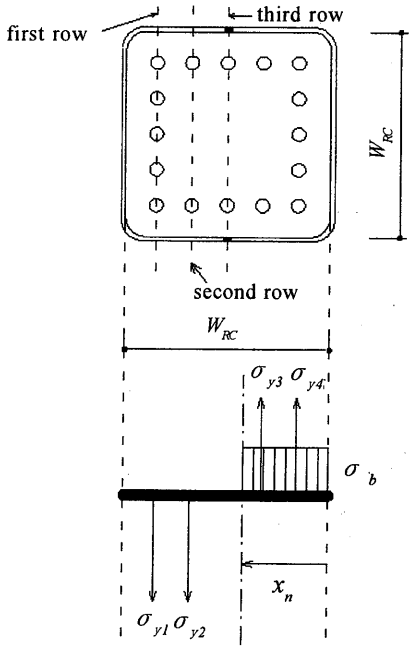

Fig.13 Stress distribution of the column base

$$M = {}_rM_u + {}_cM_u = \sum_i \sigma_{yi} \cdot A_{ri} \cdot S_{ri} + \sigma_b \cdot x_n \cdot W_{RC} \cdot 0.5 \cdot (W_{RC} - x_n) \quad (2)$$

Where,

$_rM_u$: Bending moment shared by the reinforcements

$_cM_u$: Bending moment shared by the concrete

σ_{yi} : Yield stress of the reinforcements

S_{ri} : Distances between the center of the reinforcements and the centroidal axis

A_{ri} : Cross sectional area of the center of the reinforcements

σ_b : Concrete strength considering the confining effect

x_n : Distance between the edge of the RC cross section and the neutral axis, which is calculated in accordance with the axial force ratio

W_{RC}: Width of the RC section

Table 3 Comparison of experimental and calculated ultimate bending strengths

Specimen	n	Bending moment(kN·m)			$M_{exp}/{}_cM_{cal}$	$M_{exp}/{}_BM_{cal}$
		M_{exp}	$_cM_{cal}$	$_BM_{cal}$		
No.1	0	319	364	299	0.88	1.07
No.2	0.25	388	479	426	0.81	0.91
No.3	0.5	417	461	429	0.90	0.97

RC cross section which consists of the concrete and the built-in reinforcements, as shown in Fig.13. The RC cross section is taken as the quadrangle with the width of W_{RC}. The cross section is considered as under the full plastic condition, and the stress of the third row reinforcements is omitted. The infilled concrete strength is estimated by considering the confining effect.

4.6.2 Results

Table 3 shows the comparison between the experimental and calculated ultimate bending strengths for the CFT column shafts and CFTR column bases. In Table 3, the term ${}_{C}M_{cal}$ represents the calculated ultimate bending strength of the CFT column shaft, ${}_{B}M_{cal}$ represents the calculated ultimate bending strength of the CFTR column base, M_{exp} represents the experimental ultimate bending strength. The M_{exp} is defined as the strength when the tangent stiffness is 1/6 of the initial stiffness in the *M-R* curve[6]. All the experiments results are smaller than the calculated results of the CFT column shaft. Also, it is confirmed that the experimental ultimate bending strengths favorably compare with the calculated ultimate bending strengths.

5. CONCLUSIONS

An experimental study was carried out on the non base-plate square CFTR column bases. The following conclusions can be drawn from this study:

1. The hysteretic loops of *M-R* relationships were stable and the bending moment *M* does not degrade rapidly within 3.0% of the amplitude of the *R*.
2. According to the distribution in the longitudinal direction of the bending moment components shared by the steel tubes, infill concrete and built-in reinforcements, it is confirmed that the reinforcements and rib plates play a leading role in the stress transfer and the stress can be transferred from the steel tube to the RC foundation in a convincing way.
3. The method for calculating the ultimate bending strength of the column bases is proposed and the experimental ultimate bending strengths favorably compare with the calculated results .

From above, the square CFTR column bases proposed in this study are proved to have excellent seismic performances and are applicable in the practical structural design.

ACKNOWLEDGEMENTS

This research is supported by the Japan Society for the Promotion of Science under Grant No.22360229. Also, the steel materials in this research were provided by the Okabe Corporation and Asahi Kasei Construction Materials Corporation. The supports are gratefully acknowledged.

Also, the authors appreciate the advices from K.Kutani (Professor of Kyushu Sangyo University).

REFERENCES

1) Qiao, Q.Y., et al. : A Study on the Connection of Concrete Filled Steel Tubes (CFT) with built-in Steel Bars, Proceedings of the Sixth International Conference On Behaviour of Steel Structures in Seismic Areas (STESSA 2009), Philadelphia, pp. 319-324, 2009

2) Qiao, Q.Y., et al. : Pure Bending Test on square concrete Filled Steel Tube with Built-in high strength Reinforcements(CFTR)Column Joint, Proceedings of the 4th International Conference on Steel & Composite Structures, Sydney, 2010 (CD-rom)

4) Qiao, Q.Y., et al. :Experimental Study on Mechanical Behavior of Square CFT Column Base with Built-in Reinforcements, Proceedings of the ninth Pacific Structural Steel Conference , Beijing, pp. 806-814, 2010.10

4) Kuroki, F., et al. : Experimental Study on Structural Behavior of Circular CFT Column Base with High Strength RE-Bars, Proceedings of the 8th symposium on Research and Application of Hybrid and Composite Structures, No.14, 2009.11(in Japanese)

5) AIJ: Recommendations for Design and Construction of Concrete Filled Steel Tubular Structures, 2008 (in Japanese)

6) Tateyama, E., Inoue K., Sugimoto, S., Matsumura, H. : Study on Ultimate Bending Strength and Deformation Capacity of H-shaped Beam Connected to RHS Column With Through Diaphragms, Journal of Structural and Construction Engineering, AIJ, No.389, pp. 109-121, 1988 (in Japanese)

（受理：平成23年6月2日）